*CHEMISTRY JOURNAL OF MOLDOVA. General, Industrial and Ecological Chemistry.* *2018, 13(1), 46-53*
*ISSN (p) 1857-1727 ISSN (e) 2345-1688*
*http://cjm.asm.md*
*http://dx.doi.org/10.19261/cjm.2018.483*

# HETEROTRINUCLEAR [$Fe_2^{III}Ni^{II}$]-$\mu_3$-OXO-CLUSTER BASED ON SALICYLIC ACID. SYNTHESIS, STRUCTURE AND PHYSICO-CHEMICAL PROPERTIES

Viorina Gorinchoy [a*], Vera Zubareva [a], Elena Melnic [b], Victor Kravtsov [b]

[a]*Institute of Chemistry, 3, Academiei str., Chisinau MD 2028, Republic of Moldova*
[b]*Institute of Applied Physics, 5, Academiei str., Chisinau MD 2028, Republic of Moldova*
[*]*e-mail: viorina@inbox.ru*

**Abstract.** The reaction of iron nitrate and nickel chloride with ammonium salicylate in the presence of methanol and dimethylformamide (DMF) results in the formation of a new trinuclear heterometallic complex [hexa- $\mu_2$-salicylato- $\mu_3$-oxo-(methanol) (dimethylformamide) aquadiiron(III) nickel(II)] methanol dimethylformamide. The complex crystallizes in the monoclinic space group *C*2/*c* and was structurally characterized by single crystal X-ray diffraction as $[Fe_2NiO(SalH)_6(CH_3OH)(DMF)(H_2O)]\cdot DMF\cdot CH_3OH$, where SalH are monodeprotonated salicylic acid ions. The IR and Mössbauer spectra and thermal properties were studied. The parameters of the Mössbauer spectrum ($\delta_{Fe}$= 0.45 mm/s, $\Delta E_Q$= 1.086 mm/s, 300 K) suggest the high-spin state of the $Fe^{3+}$ ions (S= 5/2).

**Keywords:** heterotrinuclear $\mu_3$-oxo complex, X-ray, IR analysis, Mössbauer spectrum, TG data.

*Received: 30 March 2018/ Revised final: 15 May 2018/ Accepted: 15 May 2018*

## Introduction

Nowadays, the field of homo- and hetero-$\mu_3$-oxo-carboxylates is one of the fastest growing areas of coordination chemistry. The area of homo- and heteropolynuclear iron carboxylate clusters are of current interest, because they may serve as versatile molecular building blocks for the design of polymeric metal-organic materials (MOM) that are amenable to crystal engineering design strategies [1-3].

Compounds of this class of substances may serve as precursors of nanooxides and metallic particles with useful magnetic properties [4,5]; they can also be used as physiologically active substances [6-10]. In addition, polynuclear clusters can give their inherent physical characteristics, such as magnetic properties, to the polymeric network, which may expand the range of potential practical applications, for example, as porous materials and magnetic sensors [11-13]. The number of iron $\mu_3$-oxo-carboxylates can be significantly expanded due to the diversity of the carboxylic ions employed as ligands and the possibility to obtain heteronuclear clusters.

Salicylic acid may be fully or partially deprotonated in solution and therefore can act as a monodentate, chelating bidentate, or bridging ligand [14]. For instance, in a dimeric terbium complex [bis(1,10-phenanthroline)tetrakis($\mu_2$-salicylato-O,O`)bis(salicylato-O,O`)(salicylato-O)diterbium] dihydrate, the salicylate ligand has been found to coordinate in three different ways [15].

Iron(III) oxide in all its forms is one of the most used metal oxide with various applications in many scientific and industrial fields. According to specialized literature, most often iron oxides are obtained from iron salts, however the use of iron homo- and heteronuclear clusters as precursors of nano-sized iron oxides is less studied. Recently, our colleagues have managed to synthesize iron oxides from heteronuclear iron clusters [16,17].

Among the metal complexes with salicylic acid deposited to the Cambridge Crystallographic Data Collection there are two iron(III) $\mu_3$-oxo-carboxylates, which were obtained in our laboratory [18]. In this article, we report a new trinuclear heterometallic complex $[Fe_2NiO(SalH)_6(CH_3OH)(DMF)(H_2O)]\cdot DMF\cdot CH_3OH$. The synthesis, crystal structure, IR, Mössbauer spectra and thermal properties were investigated and discussed. The given compound was synthesized for the purpose of obtaining raw materials for further synthesis of nanoparticles.

## Experimental

### *Synthesis of $[Fe_2NiO(SalH)_6(CH_3OH)(DMF)(H_2O)]\cdot DMF\cdot CH_3OH$*

A solution of $NiCl_2\cdot 6H_2O$ (1.15 g, 4.8 mmol) in methanol (12 mL) was added to ammonium salicylate (1.5 g, 9.68 mmol) in methanol (10 mL). The mixture was refluxed for ~1 h, whereupon a solution of $Fe(NO_3)_3\cdot 9H_2O$ (0.49 g, 1.2 mmol) in a mixture of methanol (10 mL) and DMF (1.5 mL) was added. Heating was continued, while stirring the mixture until light-green flakes dissolved. This resulted in the formation of a crystalline solid, which dissolved completely after another hour of heating. The resulting red-brown solution was transferred to a warm beaker and left overnight for crystallization. The next day, single crystals suitable for X-ray diffraction analysis were separated from the solution, while the mass product was filtered off, washed with methanol (2 mL) and dried in air. Yield: 0.59 g (77.63% relative to the iron salt).

The results of elemental analysis: Found, %: C 47.69; H 4.48; N 2.10; Ni 4.28; Fe 8.31. Calculated for $C_{50}H_{56}Fe_2Ni_1N_2O_{25}$, %: C 47.88; H 4.50; N 2.23; Ni 4.67; Fe 8.89.

The molecular formula of the mass product differs from the molecular formula of the single X-ray crystal only by one water molecule.

IR ($\upsilon$, $cm^{-1}$): 3466.9 sh, 3093.8 vw, 3050.0 vw, 1659.2 m, 1627.1 s, 1599.2 s, 1483.7 vw, 1455.7 vs, 1409.9 vw, 1392.5 vs, 1377.5 w, 1312.0 w, 1247.0 vs, 1223.1 vw, 1160.3 m, 1147.9 m, 1113.2 s, 1062.0 w, 1032.0 s, 956.7 w, 865.3 s, 811.4 vs, 758.6 vs, 722.4 w, 701.9 s, 669.1 s, 604.1 s, 560.3 vs, 532.3 w, 493.5 s, 432.2 vs (vs= very strong, s= strong, m= medium, w= weak, vw= very weak and sh= shoulder).

### *Measurements*

*X-ray diffraction analysis.* The X-ray data were collected at room temperature on an Oxford Diffraction Xcalibur diffractometer equipped with CCD area detector and a graphite monochromator utilizing MoK$\alpha$ radiation. The crystals were placed at 41 mm from the CCD detector. The data were processed using the CrysAlis package of Oxford Diffraction [19]. The final unit cell dimensions were obtained and refined on an entire data set. The structures were solved by direct methods using SHELX-97 program package [20] and refined with full-matrix least squares method with anisotropic thermal parameters for the non-hydrogen atoms.

The refinement revealed that the external apical positions at the Fe atoms are statistically occupied by water and DMF molecules with equal probability. The SalH ligands are also disordered over two positions with equal probability. Hydrogen atoms attached to carbon atoms were placed in geometrically idealized positions and refined by using a riding model. The positions of hydrogen atoms on oxygen atoms were localized on differential Fourier map add refined using restrains. The figures were produced using MERCURY [21]. CCDC 1830865 contains the crystallographic data for **1**. These data can be obtained free of charge *via* www.ccdc.cam.ac.uk/data_request/cif, or by emailing data_request@ccdc.cam.ac.uk, or by contacting The Cambridge Crystallographic Data Centre, 12 Union Road, Cambridge CB2 1EZ, UK; fax: +44 1223 336 033.

The *IR spectrum* was recorded on a Specord M75 spectrometer in the 400–4000 $cm^{-1}$ range and a Perkin-Elmer 100 FT-IR spectrometer.

The complex was analyzed for C, H, and N on a Vario EL (III) Elemental Analyzer.

Integrated *thermal analysis* was carried out on a Paulik–Paulik–Erdey derivatograph in air with $Al_2O_3$ as a reference. The recording conditions were 1/5 (DTG), 1/10 (DTA), and 100/100 (TG), $T_{max}$= 1000°C, heating rate 5°C/min, sample weight 50 mg.

The *Mössbauer spectrum* was acquired using a conventional spectrometer in the constant-acceleration mode (MS4, Edina, USA) equipped with a $^{57}Co$ source (3.7 GBq) in a rhodium matrix. The powdered sample, containing 8-10 $mg/cm^3$ of natural iron, was mounted on the plastic cell, and the spectrum was taken at room temperature (RT). Isomer shifts are quoted relative to alpha-Fe at room temperature. The spectra were fitted using the WMOSS Mössbauer Fitting Program.

## Results and discussion

### *Crystal structure*

We have shown previously that heterotrinuclear complexes with salicylic acid can be prepared by mixing a solution of iron nitrate either with solutions of different metal salicylates, or with simple metal salts in the presence of ammonium salicylate [22]. A new trinuclear heterometallic complex [hexa- $\mu_2$-salicylato- $\mu_3$-oxo-(methanol)(dimethyl formamide) aquadiiron(III) nickel(II)] methanol dimethylformamide with the composition $[Fe_2NiO(SalH)_6(CH_3OH)(DMF)(H_2O)]\cdot DMF\cdot CH_3OH$ was prepared from $Fe(NO_3)_3\cdot 9H_2O$, $NiCl_2\cdot 6H_2O$ and ammonium salicylate, at the ratio 1:4:8, respectively. The reaction was carried

out in methanol at reflux in the presence of a small amount of DMF. It was found that the presence of DMF influences the formation of the crystalline product. A significant excess of divalent nickel ions over ferric ions (4:1) is required to introduce nickel atoms into the trimer structure. The coordinating affinity of the possible apical neutral ligands (water, methanol, DMF) looks to be the same. The formation of a crystalline product is well reproducible only in the presence of a small amount of DMF. The novel heterotrinuclear cluster featuring a $\{Fe_2^{III}Ni^{II}(\mu_3\text{-}O)\}$ core and salicylate ligands (Figure 1) has been structurally characterized by single crystal X-ray diffraction analysis.

The data obtained from the X-ray analysis, as well as refinement details for the complex are summarized in Table 1, the selected geometric parameters are given in Table 2, and parameters of hydrogen bonds are presented in Table 3.

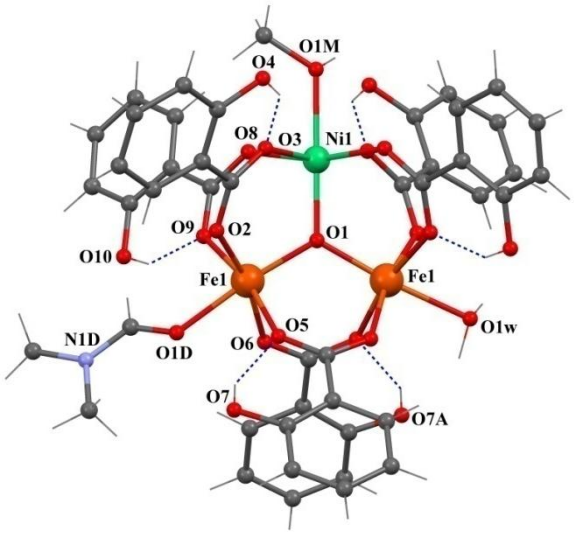


**Figure 1. Molecular structure of $[Fe_2NiO(SalH)_6(CH_3OH)(DMF)(H_2O)]$ heterocluster. Only one position of disordered moieties is shown for clarity.**

*Table 1*

**Crystallographic parameters and the data collection statistics for complex $[Fe_2NiO(SalH)_6(CH_3OH)(DMF)(H_2O)]\cdot DMF\cdot CH_3OH$.**

| *Parameter* | *Value* |
|---|---|
| Empirical formula | $C_{50}H_{54}Fe_2N_2NiO_{24}$ |
| Formula weight, M | 1237.36 |
| Temperature (K) | 293 |
| Crystal system | Monoclinic |
| Space group | *C*2/*c* |
| *Z* | 4 |
| *a* (Å) | 11.4358(13) |
| *b* (Å) | 24.153(2) |
| *c* (Å) | 22.064(2) |
| α (°) | 90 |
| β (°) | 95.010(9) |
| *γ* (°) | 90 |
| *V*, (Å$^3$) | 6070.8(9) |
| $D_{calc}$ (g cm$^{-3}$) | 1.354 |
| M (mm$^{-1}$) | 0.855 |
| *F*(000) | 2560 |
| Refinement method | Full-matrix least-squares on $F^2$ |
| *θ* Range for data collection (°) | 3.098 - 25° |
| Limiting indices | -13≤*h*≤13<br>-17≤*k*≤28<br>-15≤*l*≤26 |
| Reflections collected | 9273 |
| Reflections with [$I>2\sigma(I)$] | 5299 [$R_{(int)}$ = 0.0429] |
| Data/restraints/parameters | 5299 / 362 / 421 |
| Goodness-of-fit on $F^2$ | 1.002 |
| $R_1$ | $R_1$= 0.0855 |
| w$R_2$ [$I>2\sigma(I)$] | $wR_2$= 0.2075 |
| $R_1$ | $R_1$= 0.1695 |
| w$R_2$ (all data) | $wR_2$= 0.2540 |
| Largest difference in peak and hole (e Å$^{-3}$) | 0.571 and -0.495 |

*Table 2*

**Selected bond lengths and bond angles in the coordination sphere of each metal atom.**

| *Bond* | *d*, Å | *Bond* | *d*, Å |
|---|---|---|---|
| Fe1-O1 | 1.887(3) | Ni1-O1 | 1.885(5) |
| Fe1-O9 | 2.024(4) | Ni1-O8 | 2.017(5) |
| Fe1-O2 | 2.032(4) | Ni1-O3 | 2.042(5) |
| Fe1-O5[1] | 2.051(5) | Ni1-O1M | 2.104(7) |
| Fe1-O6 | 2.058(5) | Ni1-Fe1 | 3.261(1) |
| Fe1-O1D | 2.096(12) | Fe1-Fe1 | 3.277(2) |
| Fe1-O1*w* | 2.153(14) | | |
| *Angle* | *ω, deg* | *Angle* | *ω, deg* |
| O1-Fe1-O9 | 95.9(2) | O6-Fe1-O1*w* | 89.2(4) |
| O1-Fe1-O2 | 96.0(2) | O9-Fe1-O2 | 91.9(2) |
| O1-Fe1-O5[1] | 96.0(2) | O9-Fe1-O5[1] | 168.1(2) |
| O1-Fe1-O6 | 95.1(2) | O9-Fe1-O6 | 88.7(2) |
| O1-Fe1-O1D | 172.4(3) | O9-Fe1-O1D | 84.7(4) |
| O1-Fe1-O1*w* | 174.9(4) | Fe1[1]-O1-Fe1 | 120.6(3) |
| O2-Fe1-O5[1] | 88.5(2) | O1-Ni1-O8 | 96.6(1) |
| O2-Fe1-O6 | 168.8(2) | O1-Ni1-O3 | 96.3(1) |
| O2-Fe1-O1D | 91.6(3) | O1-Ni1-O1M | 180.0 |
| O2-Fe1-O1*w* | 79.9(4) | O3-Ni1-O1M | 83.7(1) |
| O5[1]-Fe1-O6 | 88.6(2) | O8-Ni1-O3 | 90.9(2) |
| O5[1]-Fe1-O1D | 83.4(4) | O8-Ni1-O1M | 83.4(1) |
| O5[1]-Fe1-O1*w* | 86.9(5) | Ni1-O1-Fe1 | 119.7(1) |
| O6-Fe1-O1D | 77.4(3) | | |

*Symmetry transformations used to generate equivalent atoms*: [1)] *-x, y, -z*+1/2

*Table 3*

**Hydrogen bond distances (Å) and angles (°).**

| *D-H···A* | *d(H···A)* | *d(D···A)* | *< (DHA)* |
|---|---|---|---|
| O4─H4···O3 | 0.82 | 1.83 | 2.538(8) |
| O4A─H4A···O2 | 0.82 | 1.78 | 2.50(3) |
| O7─H7···O6 | 0.82 | 1.80 | 2.528(11) |
| O7A─H7A···O5 | 0.82 | 1.80 | 2.52(2) |
| O10A─H10A···O8 | 0.82 | 1.91 | 2.584(13) |
| O10─H10···O9 | 0.82 | 1.77 | 2.497(13) |

The trinuclear cluster resides on two fold crystallographic axis passing through O1, Ni1, and O1m atoms, thus having $C_2$ molecular symmetry. In the structure of this complex, one $Ni^{2+}$and two $Fe^{3+}$ ions occupy the vertexes of about equilateral triangle, Fe···Fe and Ni···Fe distances equal 3.277(2) Å; 3.261(1) Å, respectively (Table 2). The centre of the triangle is occupied by the $\mu_3$-O atom which is coplanar with the metal atoms. The metal ions have an octahedral coordination but a different environment. The coordination sphere of each metal atom is constituted from four O atoms of four bridging salycilates, central $\mu_3$-oxo atom and apical ligand. The external apical position of Fe ions is statistically occupied with equal probability by a DMF or water molecule, while the Ni ion is capped in the apical position by the methanol molecule, which is also disordered over two positions in accordance with $C_2$ symmetry. The position of SalH ligands in the complex is stabilized by intramolecular O─H···O hydrogen bonds (Table 2). The crystal structure is stabilized by intermolecular $\pi$–$\pi$ stacking interactions between parallel, centre symmetry related aromatic C6 rings of SalH ligands with centroid···centroid separation of 3.760 and 4.548 Å (Figure 2).

***Infrared spectroscopy***

The IR spectrum of the solid salicylate complex can be divided into several regions: 3466.9-3000 $cm^{-1}$ is attributed to the stretching absorption of the OH-groups originated from water, methanol molecules, and from phenol groups (salicylate anions); 2000-1659.2 $cm^{-1}$, combined vibrations; 1659.2-1377.5 $cm^{-1}$, involving both the C-O stretching of the carboxyl group and aromatic C-C stretching vibrations; 1377.5-1312.0 $cm^{-1}$, the C-O-H bending of the phenol groups; 1247.0-1223.1 $cm^{-1}$, stretching of

the phenol groups; 1160.3-1032.0 $cm^{-1}$, bending in the C-H-C plane in the substituted aromatic rings; 865.3-811.4 $cm^{-1}$, scissoring vibrations in the carboxyl groups; 758.6-722.4 $cm^{-1}$, out of plane bending of hydrogen atoms in the benzene rings; and 700-400 $cm^{-1}$, bending in the benzene rings [14,23,24].

The IR spectrum contains absorption bands at 669.1-432.2 $cm^{-1}$, which can be assigned to *ν*(FeO) and *ν*(NiO) stretching vibrations [14].

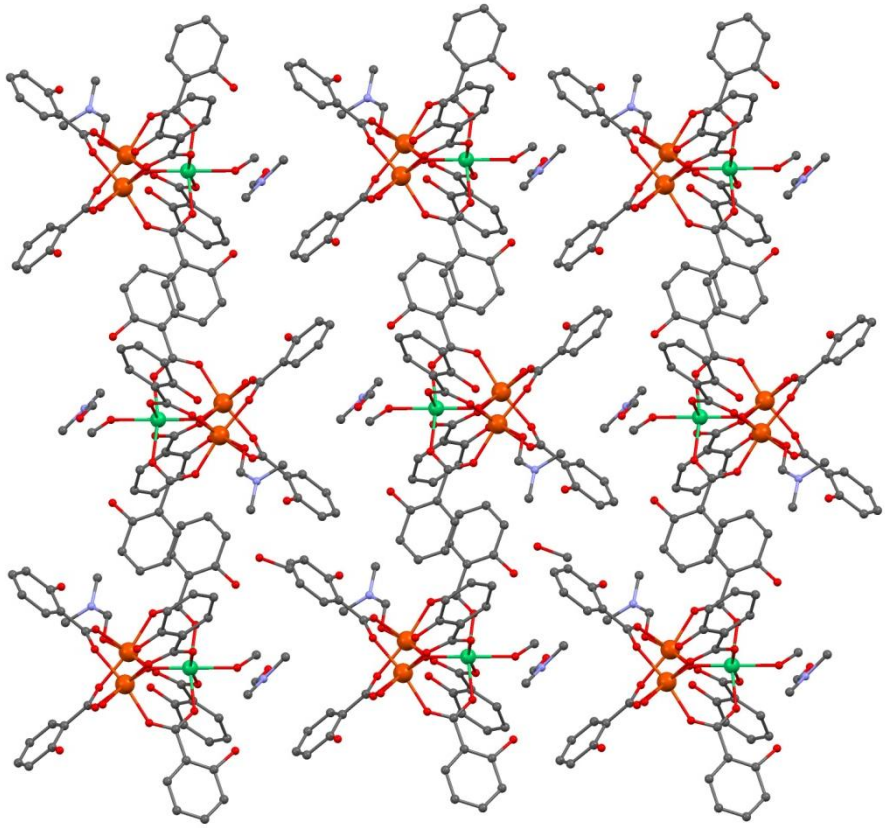

**Figure 2. Fragment of the crystal structure of the complex $[Fe_2NiO(SalH)_6(CH_3OH)(DMF)(H_2O)]\cdot DMF\cdot CH_3OH$.**

***Thermogravimetric analysis***

The thermo-gravimetric curves of the $[Fe_2NiO(SalH)_6(CH_3OH)(DMF)(H_2O)]\cdot DMF\cdot CH_3OH$ complex are presented in Figure 3 demonstrating that the complex is thermally unstable. The thermolysis process begins at 37.5°C and involves many steps; the DTG and TG curves suggest that the first process at 37.5–110°C is endothermic and corresponds to a weight loss of ~4%. It seems to be highly probable that the observed change is attributable to the elimination of a methanol ($CH_3OH$) molecule. Subsequent processes endo- at 110–176°C (II), exo- 176–260°C (III), exo- 260–320°C (IV) and exo- 320–500°C (V) are due to the elimination of all solvent molecules and destruction of remaining organic ligands (Table 4). The final thermolysis product consists of ~18% of the initial weight, which corresponds to the mixed oxide formation, $Fe_2O_3\cdot NiO$ (calculated: 18.94%). Schematically, the decomposition of the complex may be presented by the following steps (Table 4):

$$[Fe_2NiO(SalH)_6(CH_3OH)(DMF)(H_2O)]\cdot DMF\cdot CH_3OH \xrightarrow[-[CH_3OH]]{} \quad (I)$$

$$[Fe_2NiO(SalH)_6(CH_3OH)(DMF)(H_2O)]\cdot DMF \xrightarrow[-2[DMF]-1.5[SalH]]{} \quad (II)$$

$$[Fe_2NiO(SalH)_{4.5}(CH_3OH)(H_2O)] \xrightarrow[-[CH_3OH]-[H_2O]]{} [Fe_2NiO(SalH)_{4.5}] \quad (III)$$

$$[Fe_2NiO(SalH)_{4.5}] \xrightarrow[-[SalH]]{} [Fe_2NiO(SalH)_{3.5}] \quad (IV)$$

$$[Fe_2NiO(SalH)_{3.5}] \xrightarrow[-3.5[SalH]]{} [Fe_2O_3\cdot NiO] \quad (V)$$

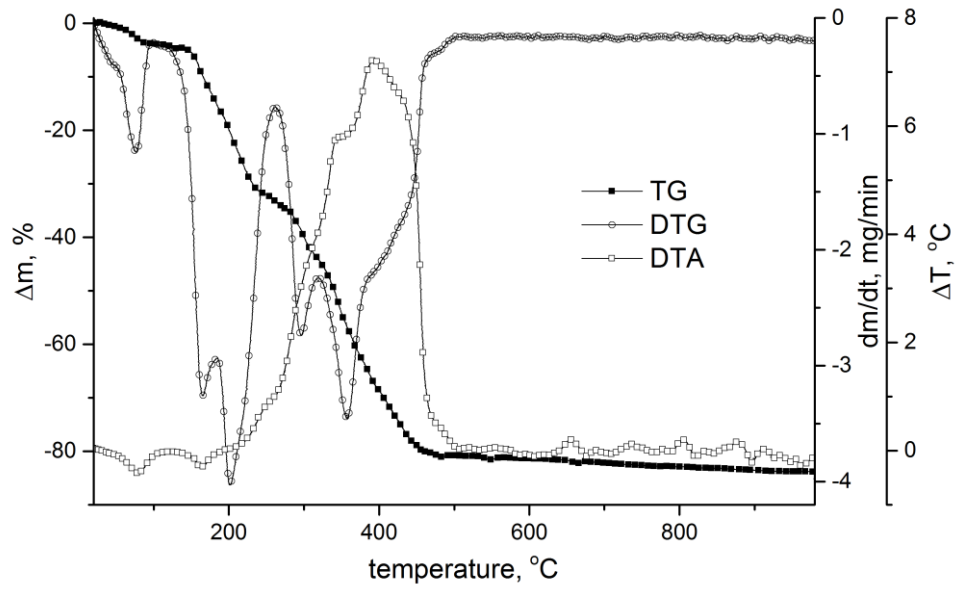


**Figure 3. Termogravimetric curves (TG, DTG, DTA) for the investigated complex.**

*Table 4*

**Thermogravimetric data for the $[Fe_2NiO(SalH)_6(CH_3OH)(DMF)(H_2O)]\cdot DMF\cdot CH_3OH$ complex.**

| *Steps* | *Effect* | *T, °C* | | | *Weight loss found, %* |
|---|---|---|---|---|---|
| | | *onset* | *maxim* | *end* | |
| I | endo | 37.5 | 75 | 110 | 4 |
| II | endo | 110 | 168 | 176 | 28 |
| III | exo | 176 | 200 | 260 | 4 |
| IV | exo | 260 | 294 | 320 | 10 |
| V | exo | 320 | 360 | 500 | 36 |

***Mössbauer spectroscopy***

The Mössbauer spectrum of the investigated complex at 300 K is presented in Figure 4. The spectrum is comprised of a doublet and on its basis were calculated the corresponding parameters (Table 5). The values of isomer shift $\delta_{Fe}$(0.45 mm/s) and quadrupole splitting $\Delta E_Q$(1.08 mm/s) correspond to iron(III) in the high spin state (S= 5/2) [25]. Table 5 exemplifies heterotrinuclear complexes with the fragment $\{Fe_2MO\}$ (where M= $Mg^{2+}$, $Co^{2+}$, $Ni^{2+}$) and the homotrinuclear cations complex $\{Fe_3O\}$. The parameters of the Mössbauer spectra of all the compounds indicate the presence of high-spin iron(III) (S= 5/2). The analysis of isomer shift values ($\delta_{Na}^{+}$) (Table 5) at 300 and 80 K shows that the monodentate ligands and $M^{2+}$ ions in the inner sphere, as well as the anion and solvent molecules in the external sphere, do not influence the total density of *s*-electrons on the nucleus [26-28]. Replacement of one iron(III) ion in the triangle by a cobalt(II), magnesium(II) or nickel(II) ion increases the quadrupole splitting from 0.76 to 1.08 mm/s. This change is consistent with our data [27] and the data obtained by other researchers [28] and is due to the lowering of the symmetry of the fragment $\{Fe_2MO\}$ in the complex from $D_{3h}$ to $C_{2v}$.

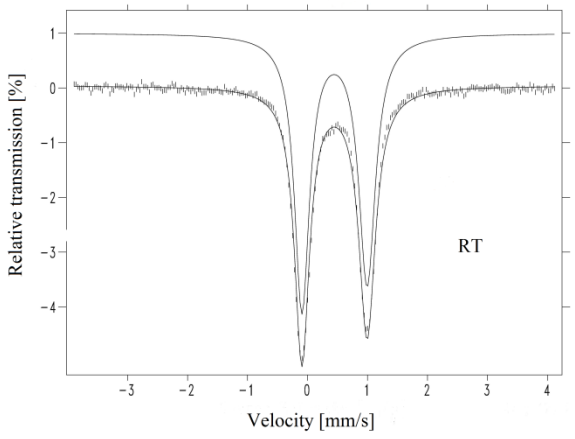


**Figure 4. Mössbauer spectrum of $[Fe_2NiO(SalH)_6(CH_3OH)(DMF)(H_2O)]\cdot DMF\cdot CH_3OH$ at room temperature.**

*Table 5*

**Parameters of the Mössbauer spectra of the obtained compound $[Fe_2NiO(SalH)_6(CH_3OH)(DMF)(H_2O)]\cdot DMF\cdot CH_3OH$ and other homo- and heterometallic iron(III) $\mu_3$-oxosalicylates.**

| *Complex* | *T, K* | *Isomer shift* ($\delta_{Na}$ *) | *Quadrupol splitting* ($\Delta E_Q$) | *Line width, (G)* | *Spin state (S)* | *Lit. ref.* |
|---|---|---|---|---|---|---|
| | | mm/s | | | | |
| $[Fe_2NiO(SalH)_6(CH_3OH)(DMF)(H_2O)]\cdot DMF\cdot CH_3OH$ | 300 | 0.45 | 1.08 | 0.32 | 5/2 | This work |
| $[Fe_2MgO(SalH)_6(DMAA)_{0.4}(H_2O)_{2.6}]\cdot 4DMAA$ | 300<br>80 | 0.71<br>0.76 | 1.08<br>1.28 | 0.26<br>0.29 | 5/2 | [16] |
| $[Fe_2CoO(SalH)_6(CH_3OH)_2(H_2O)]\cdot DMFA\cdot 2.5H_2O$ | 300<br>80 | 0.68<br>0.81 | 1.04<br>1.09 | 0.34<br>0.32 | 5/2 | [16] |
| $[Fe_3O(SalH)_6(H_2O)_3]Cl\cdot DMAA\cdot H_2O$ | 300 | 0.66 | 0.76 | 0.35 | 5/2 | [16] |

** The isomer shifts are referenced to sodium nitroprusside.*

## Conclusions

A new trinuclear heterometallic iron/nickel carboxylate complex was synthesized and characterized by IR and Mössbauer spectroscopies, TGA and single crystal X-ray analyses. The crystallographic study reveals that the complex has a typical $\mu_3$-oxo structure with three different ligands at apical positions of metal atoms (one nickel and two iron atoms). The parameters of the Mössbauer spectrum suggest the high-spin state of the $Fe^{3+}$ ions.

### References


1. Schoedel, A.; Wojtas, L.; Kelley, S.P.; Rogers, R.D.; Eddaoudi, M.; Zaworotko, M.J. Network diversity through decoration of trigonal-prismatic nodes: two-step crystal engineering of cationic metal-organic materials. Angewandte Chemie International Edition, 2011, 50(48), pp. 11421-11424. DOI: https://doi.org/10.1002/anie.201104688
2. Schoedel, A.; Zaworotko, M.J. $[M_3(\mu_3\text{-}O)(O_2CR)_6]$ and related trigonal prisms: versatile molecular building blocks for crystal engineering of metal-organic material platforms. Chemical Science, 2014, 5(4), pp. 1269-1282. DOI: 10.1039/C4SC00171K
3. Botezat, O.; van Leusen, J.; Kravtsov, V.Ch.; Filippova, I.G.; Hauser, J.; Speldrich, M.; Hermann, R.P.; Krämer, K.W.; Liu, Sh.-X.; Decurtins, S.; Kögerler, P.; Baca, S.G. Interpenetrated (8,3)-c and (10,3)-b metal–organic frameworks based on $\{Fe^{III}_3\}$ and $\{Fe^{III}_2Co^{II}\}$ pivalate spin clusters. Crystal Growth & Design, 2014, 14(9), pp. 4721–4728. DOI: 10.1021/cg5008236
4. Yang, P. Eds. The Chemistry of Nanostructured Materials. World Scientific: Hong Kong, 2003, 396 p. https://www.worldscientific.com/worldscibooks/10.1142/5304
5. Yu, W.W.; Falkner, J.C.; Yavuz, C.T.; Colvin, V.L. Synthesis of monodisperse iron oxide nanocrystals by thermal decomposition of iron carboxylate salts. Chemical Communications, 2004, 0(20), pp. 2306-2307. DOI: 10.1039/B409601K
6. Sheriff, S.; Hendrickson, W.A.; Smith, J.L. Structure of myohemerythrin in the azidomet state at 1.713 Å resolution . Journal of Molecular Biology, 1987, 197(2), pp. 273-296. DOI: https://doi.org/10.1016/0022-2836(87)90124-0
7. Syrbu, T.; Turta, C.; Gorinchoy, V.; Melnic, S.; Burteva, S., Stepanov, V. Nutrient medium for cultivation of Penicillium funiculosum CNMN FD11 fungus strain. MD Patent, 2012, No. 4158 (in Romanian).
8. Syrbu, T.F.; Turte, K.I.; Mikhailova, R.V.; Moroz, I.V.; Lobanok, A.G.; Burtseva, S.A.; Stepanov, V.S.; Gorinchoy, V.V.; Melnik, S.V. Effect of salicylate and furoate complex iron compounds on catalase production by fungi of Penicillium genius. Proceedings of the National Academy of Sciences of Belarus. Series of Biological Sciences, 2011, 3, pp. 57-61. http://nasb.gov.by/eng/publications/vestib/vbi11_3.php
9. Bulhac, I.; Ştefirta, A. Coordination compounds of some 3d-metals with biological activity. Akademos, 2011, 1(20), pp. 19-24 (in Romanian). http://www.akademos.asm.md/taxonomy/term/56
10. Ştefirta, A.; Brinza, L.; Toma, S.; Buceaceaia, S.; Melenciuc, M.; Bulhac, I.; Turta, C.; Zubareva, V.; Barba, N.; Robu, S. Dimination of the impact of extreme pedoclimatic factors on plants. Publishing House of ASM: Chisinau, 2008, pp. 166-202. (in Romanian).
11. Cannon, R.D.; White, R.P. Chemical and physical properties of triangular bridged metal complexes. Progress in Inorganic Chemistry, 2007, 36, pp. 195-298. DOI: https://doi.org/10.1002/9780470166376.ch3
12. Dulcevscaia, G.M.; Filippova, I.G.; Speldrich, M.; van Leusen, J.; Kravtsov, V.Ch.; Baca, S.G.;

Kogerler, P.; Liu, S.-X.; Decurtins, S. Cluster-based networks:1D and 2D coordination polymers based on {$MnFe_2(\mu_3$-O)}-type clusters. Inorganic Chemistry, 2012, 51(9), pp. 5110-5117. DOI: 10.1021/ic202644t

13. Liu, Yu.; Eubank, J.F.; Cairns, A.J.; Eckert, J.; Kravtsov, V.Ch.; Luebke, R.; Eddaoudi, M. Assembly of metal-organic frameworks (MOFs) based on indium-trimer building blocks: a porous MOF with soc topology and high hydrogen storage. Angewandte Chemie. International Edition, 2007, 46(18), pp. 3278-3283. DOI: https://doi.org/10.1002/anie.200604306
14. Tel'zhenskaya, P.N.; Shvarts, E.M. Complex compounds of salicylic acid and its derivatives. Russian Journal of Coordination Chemistry, 1977, 3(9), pp. 1279-1295 (in Russian). http://www.maik.ru/ru/journal/kordkhim/
15. Yin, M.; Ai, C.; Yuan, L.-J.; Wang, C.; Sun, J. Synthesis, structure and luminescent property of a binuclear terbium complex $[Tb_2(Hsal)_8(H_2O)_2][(Hphen)_2]\cdot 2H_2O$. Journal of Molecular Structure, 2004, 691(1-3), pp. 33-37. DOI: https://doi.org/10.1016/j.molstruc.2003.10.032
16. Turta, C.; Melnic, S.; Prodius, D.; Macaev, F.; Stoeckli-Evans, H.; Ruiz, P.; Muraviev, D.; Pogrebnoi, S.; Ribkovskaia, Z.; Mereacre, V.; Lan, Y.; Powell, A.K. Sunflower oil coating on the nanoparticles of iron (III) oxides. Inorganic Chemistry Communications, 2010, 13(12), pp. 1402-1405. DOI: https://doi.org/10.1016/j.inoche.2010.07.046
17. Iacob, M.; Cazacu, M.; Racles, C.; Ignat, M.; Cozan, V.; Sacarescu, L.; Timpu, D.; Kajňaková, M.; Botko, M.; Feher, A.; Turta, C. Iron-chromium oxide nanoparticles self-assembling into smectic mesophases. RSC Advances, 2014, 4(12), pp. 6293-6299. DOI: 10.1039/c3ra47072e
18. Gorinchoy, V.V.; Zubareva, V.E.; Shova, S.G.; Szafranski, V.N.; Lipkowski, J.; Stanica, N.; Simonov, Yu.A.; Turta, C.I. Homo- and heteronuclear iron complexes $\{Fe_2MO\}$ with salicylic acid: Synthesis, structures, and physicochemical properties. Russian Journal of Coordination Chemistry, 2009, 35(10), pp. 731-739. DOI: https://doi.org/10.1134/S1070328409100042
19. *CrysAlis*PRO: Agilent Technologies Ltd: Yarnton, Oxfordshire, England, 2014. https://www.agilent.com/search/?Ntt=CrysAlisPRO
20. Sheldrick, G.M. A short history of *SHELX*. Acta Crystallographica Section A, 2008, A64, p. 112-122. DOI: https://doi.org/10.1107/S0108767307043930
21. Macrae, C.F.; Edgington, P.R.; McCabe, P.; Pidcock, E.; Shields, G.P.; Taylor, R.; Towler, M.; van de Streek, J. Mercury: visualization and analysis of crystal structures. Journal of Applied Crystallography, 2006, 39, pp. 453-457. DOI: http://dx.doi.org/10.1107/S002188980600731X
22. Melnic, E.; Gorinchoy, V.; Zubarev, V.E.; Kravtsov, V.Ch. X-Ray study of novel heterotrinuclear $(Fe_2^{III}Ni^{II})$-$\mu_3$-oxo clusters based on salicylic acid $[Fe_2NiO(SalH)_6(CH_3OH)(DMF)(H_2O)]$ $(DMF)(CH_3OH)$. The 6th International Conference on Materials Science and Condensed Matter Physics MSCMP. Chisinau, 2012, p. 92.
23. Introduction to Spectroscopy – Chemistry https://www2.chemistry.msu.edu/faculty/reusch/virttxtjml/spectrpy/infrared/infrared.htm
24. Nakomoto, K. Infrared and Raman Spectra of Inorganic and Coordination Compounds, Part A: Theory and Applications in Inorganic Chemistry, 6th Edition. John Wiley & Sons Inc., Hoboken: New Jersey, 2009, 432 p. https://www.wiley.com/
25. Goldanskii, V.I.; Herber, R.H. Chemical applications of Mössbauer spectroscopy. Academic Press: New York and London, 1968, 701 p.
26. Gorinchoy, V.; Shova, S.; Melnic, E.; Kravtsov, V.; Turta, C. Homotrinuclear $Fe_3^{III}$ $\mu$ – oxo salicylate cluster. Synthesis, structure and properties. Chemistry Journal of Moldova, 2013, 8(2), pp. 83-89. DOI: dx.doi.org/10.19261/cjm.2013.08(2).10
27. Melnic, S.; Prodius, D.; Stoeckli-Evans, H.; Shova, S.; Turta, C. Synthesis and anti-tuberculosis activity of new hetero(Mn, Co, Ni)trinuclear iron(III) furoates. European Journal of Medicinal Chemistry. 2010, 45(4), pp.1465-1469. DOI: https://doi.org/10.1016/j.ejmech.2009.12.053
28. Melnic, S.; Prodius, D.; Simmons, Ch.; Zosim, L.; Chiriac, T.; Bulimaga, V.; Rudic, V.; Turta, C. Biotechnological application of homo- and heterotrinuclear iron(III) furoates for cultivation of iron-enriched *Spirulina*. Inorganica Chimica Acta, 2011, 373(1), pp.167-172. DOI: https://doi.org/10.1016/j.ica.2011.04.011